Self-Similar Tip Growth in Filamentary Organisms

Alain Goriely* and Michael Tabor†

Program in Applied Mathematics, University of Arizona, Tucson, Arizona 85721

(Received 12 September 2002; published 13 March 2003)

The growth of a family of filamentary microorganisms is described in terms of self-similar growth at the tip which is driven by pressure and sustained by a wall-building growth process. The cell wall is modeled biomechanically as a stretchable elastic membrane using large-deformation elasticity theory. Incorporation of geometry dependent elastic moduli and a self-similar ansatz shows how these equations can generate realistic tip shapes corresponding to a self-similar expansion process.

DOI: 10.1103/PhysRevLett.90.108101 PACS numbers: 87.18.La, 46.70.Hg

Tip growth and the evolution of fingerlike and filamentary structures, such as occur in the Hele-Shaw cell and dendritic growth, have long been topics of interest in condensed matter physics [1]. The purpose of this Letter is to describe a family of microorganisms, the prokaryotic actinomycetes, that grow as fingerlike structures in which the growth activity is concentrated at the tip. Analogies with the above-mentioned physical problems are tantalizing but, as will be described, the growth process requires very different modeling assumptions.

An important member of the actinomycete family are the streptomycetes which are of great interest in the pharmaceutical industry because of their ability to generate antibiotics. In a typical growth cycle, spores bud into long filamentary hyphae which grow in and on the nutrient surface. The hyphae undergo branching and a dense colony is gradually formed. This phase is usually referred to as the vegetative growth phase. The antibiotics are produced in a subsequent aerial growth phase. Experimental studies [2] have clearly demonstrated that the vegetative growth is apical, i.e., occurs at the tip of the hyphae through a complex process in which wall-building polymers are incorporated into the tip which is stretched by the turgor pressure generated by the cytoplasm inside the cell. As the tip is continually stretched and "rebuilt," the more distant portions of the hyphal wall rigidify. The net result is a (steadily) propagating fingerlike structure. A typical time-lapsed hyphal growth sequence is shown in Fig. 1.

A typical streptomycete filament, such as *Streptomyces coelicolor*, is less than 1 μm in diameter and can grow to lengths of 50–100 μm in the vegetative phase. Another broad family of microorganisms, the eukaryotic fungi—which are typically an order of magnitude bigger than the actinomycetes—are also observed to undergo apical hyphal growth. However, as eukaryotes, they have a much more complex internal cell structure and different wall composition than the actinomycetes. For the latter organisms, it is generally accepted that turgor pressure is the primary driving force and that wall-building materials are probably transported to the tip by some form of diffusive process. In the case of fungi, the role of turgor pressure is still being debated [3] and the cytoskeleton almost certainly plays some role in straining the cell membrane and transporting the wall-building materials to the tip.

The modeling of tip growth in both families of organisms has inevitably been a topic of interest for some time. Most models have been geometric in nature, attempting to balance the increase in wall area of an advancing membrane "front" with the incorporation of wall-building material. Some of these models [4] assume a given tip shape and others attempt to deduce it in the particular case of fungal growth [5]. Other models for actinomycetes [6], based on the Young-Laplace law for membranes, suggest connections between experimentally observed tip shapes and their material properties. However, the common feature of these approaches is that they either assume, or attempt to identify, an explicit form for the tip shape. Here we concentrate on the turgor pressure driven apical growth of actinomycetes and, using large-deformation elasticity theory [7], develop a self-consistent biomechanical model in which the cell wall is modeled as a stretchable and growing elastic membrane with geometry dependent moduli. Our results show that there is not so much one special tip shape but rather that the tip expansion is essentially *self-similar*. Governing equations for such self-similar tip shapes are derived and

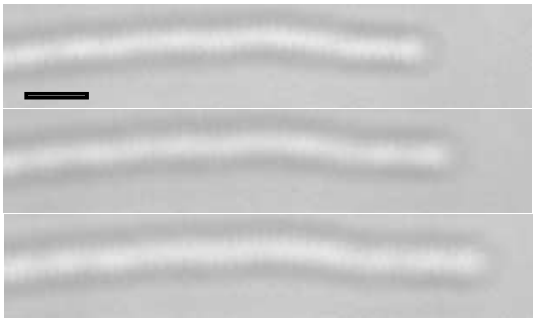

FIG. 1. Time lapsed sequence of hyphal growth of *Streptomyces coelicolor* A3(2). Each image is 150 sec apart (bar is 1 μm). Images collected courtesy Arizona Research Laboratory.

solved numerically and analytically. We comment that other modeling approaches, such as the use of curve dynamics techniques that have been applied to the physical problems mentioned at the beginning of this Letter, are attractive but must be treated with caution when trying to model the real biological process. This topic is explored elsewhere [8].

In our model, the filament is assumed (as it is in all the earlier models cited above) to be in the form of an axisymmetric surface of revolution. Distance along the membrane is parametrized in terms of the material coordinate, σ, and the shell itself is characterized by the two variables $r = r(\sigma)$ and $\theta = \theta(\sigma)$ as shown in Fig. 2. The deformation of the membrane is described by the two deformation order parameters,

$$\lambda_\varphi = \frac{r(\sigma)}{r_0(\sigma)}, \qquad \lambda_s = \frac{ds}{d\sigma},$$

where λ_φ measures the radial expansion of a given material point with respect to the reference configuration r_0, and the metric λ_s measures the longitudinal extension of that point under deformation. Before deformation or growth, the material parameter σ is identified with the arclength. Obviously, $\lambda_s = 1$ corresponds to no longitudinal stretching of the membrane.

If t_s and t_φ are, respectively, the longitudinal (in the direction of increasing arclength) and latitudinal (in the direction of increasing azimuthal angle) tensions on the surface, the equations of mechanical equilibrium for a surface of revolution, in which shearing and bending moments are neglected, are [9]

$$\frac{dr}{d\sigma} = \lambda_s \cos\theta, \tag{1}$$

$$\frac{dt_s}{d\sigma} = \lambda_s \frac{\cos\theta}{r}(t_\varphi - t_s) - \tau, \tag{2}$$

$$P = \kappa_s t_s + \kappa_\varphi t_\varphi, \tag{3}$$

where τ denotes any externally imposed surface stresses (henceforth taken to be zero). The last of these equations represents a generalized form of the Young-Laplace law for a membrane with principal curvatures $\kappa_s = d\theta/ds$ and $\kappa_\varphi = \sin\theta/r$ supporting a pressure difference P. The description of the curve geometry can be completed by integrating the additional equation $dz/d\sigma = \lambda_s \sin\theta$. In large-deformation theory, the strains $e_{\alpha\beta}$ for the axisymmetric configuration are quadratic functions of the deformation parameters, namely, $e_{ss} = (\lambda_s^2 - 1)/2$, $e_{\varphi\varphi} = (\lambda_\varphi^2 - 1)/2$, and here the stresses t_s and t_φ are assumed to follow the equivalent of a linear constitutive relationship of the form

$$t_s = a[\lambda_s^2 + \mu\lambda_\varphi^2 - (1 + \mu)], \tag{4}$$

$$t_\varphi = a[\lambda_\varphi^2 + \mu\lambda_s^2 - (1 + \mu)], \tag{5}$$

where μ measures the ratio of azimuthal and longitudinal stretching and a is an effective elastic modulus for the membrane. An important part of this study is to allow it to be geometry dependent, i.e., $a = a(\sigma)$. More complex forms of constitutive relationship can be used (as in studies of red blood cells [10]) but, given the current lack of detailed information about the elastic properties of actinomycete membranes, a linear relationship is more than adequate for the ensuing demonstration of self-similar expansion.

In the case of constant pressure P, the system (1)–(3) admits the conserved quantity

$$C = r^2(2t_s\kappa_\varphi - P), \tag{6}$$

where, for all solution $[r(\sigma), \theta(\sigma)]$ crossing the z axis, $C = 0$. Taking advantage of this quantity enables us to reduce the third order system to the closed second order system for the shell shape, namely,

$$\frac{dr}{d\sigma} = \lambda_s \cos\theta, \tag{7}$$

$$\frac{d\theta}{d\sigma} = \frac{-\lambda_s}{r}\frac{\sin\theta[r^2 - r_0^2(1 + \mu(1 - \lambda_s^2))] - prr_0^2}{r^2\mu - r_0^2(1 + \mu - \lambda_s^2)}, \tag{8}$$

where $p = P/a$ is an effective pressure and, assuming $C = 0$, $\lambda_s^2 = 1 + \mu[1 - (r/r_0)^2] + rp/(2\sin\theta)$.

Experimental results [11] clearly demonstrate that growth in actinomycetes takes place in the apical (tip) region where the cell wall is softer. This is modeled biomechanically by using a material dependent elastic modulus $a = a(\sigma)$. The published data on the rate of incorporation of tritiated *N*-acetyl D-glucosamine in the tip region of *S. coelicolor* A3(2) [11] can be fitted [12] by the following function, displayed in Fig. 3:

$$p = \tfrac{1}{2}A\{1 - \tanh[(\sigma - \sigma_1)/\alpha]\} + \beta, \tag{9}$$

where the parameters σ_1 and α characterize the extent of the apical extension zone. The parameter β is a small number which describes the effective pressure far from the tip, whereas $A + \beta$ gives the effective pressure at the tip.

During growth, the wall of the filament is regenerated by the incorporation of wall-building polymers

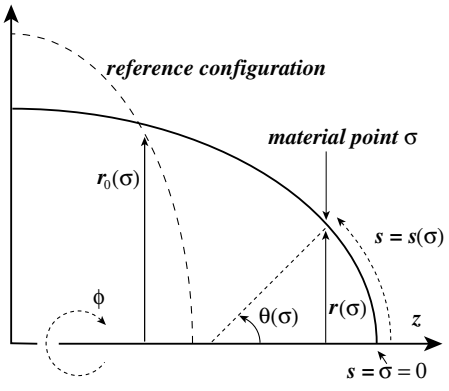

FIG. 2. Shell coordinate system for an axisymmetric shell.

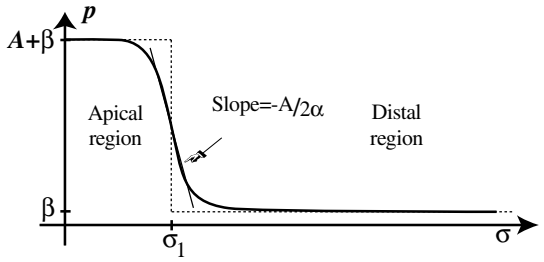

FIG. 3. The effective pressure P/a (solid line). Close to the tip (apical region), the effective pressure is high and drops off away from the tip (distal region). The idealized profile used for the theoretical analysis is shown with a dashed line.

transported to the tip. The addition of new material allows the membrane to be further stretched by the turgor stresses. This effect can be simulated by taking the deformed membrane as a new reference configuration susceptible to elastic deformation. Mathematically, this growth process is achieved by simply translating the arclength of the (quasiequilibrium) extended configuration into the new material coordinate. Thus, we start with an initial shape defined by the function $r_0(\sigma)$, $0 \leq \sigma \leq L_0$, and compute the new shape $r(\sigma)$ from (7) and (8) subject to the boundary condition $r(L_0) = R_0$, $r(0) = 0$. The new shape $r(\sigma)$ represents the new mechanical equilibrium of the membrane which is then translated into the "next" reference shape $r_1(\sigma) = r(s)$, where $s = s(\sigma)$ with $0 \leq \sigma \leq L_1 = s(L_0)$. A new mechanical equilibrium with boundary conditions $r(L_1) = R_0$, $r(0) = 0$ is then calculated, and the growth process is repeated.

A typical computation using Eqs. (7)–(9) shown in Fig. 4 illustrates the fundamental point that the tip shape, once established, is effectively self-similar, i.e., away from the fixed boundary and at each step the new shape is, essentially, an affinely translated duplicate of the previous one. The above results suggest the possibility of self-similar shell stretching and here our goal is to show how the shell equations can be developed in such a way as to produce this type of expansion. This is achieved

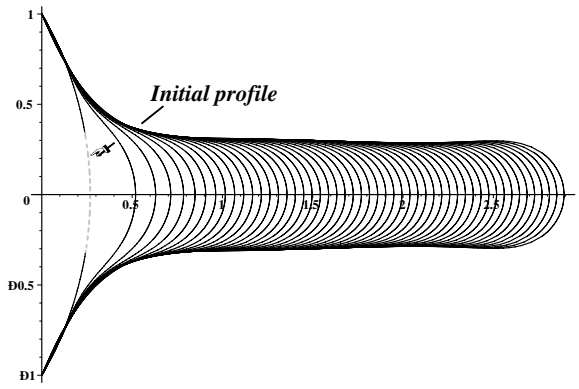

FIG. 4. A growth sequence obtained from an initial spherical shape ($\mu = 1/2$, $\sigma_1 = \pi/2$, $\beta = 10^{-6}$, $P = A = 1$, $\alpha = 1/8$, $L_1 = \pi/3$, 200 iterations, every four shown).

by adopting a picture in which self-similar tip growth is one in which the "final" tip shape, $r(\sigma)$, is of the same functional form as the initial "reference" configuration $r_0(\sigma)$. The key idea, as illustrated in Fig. 5, is quite simply to set

$$r(\sigma) = r_0[s(\sigma)]. \tag{10}$$

That is, after expansion the value of the radial variable, r, for a given material point σ is required to be the value of r_0 evaluated at the new position of that point, expressed in terms of arclength, along the shell. The angular deformation variable, λ_φ, now takes the form $\lambda_\varphi = r_0[s(\sigma)]/r_0(\sigma)$. This form is well suited for hyphal growth since far from the tip we expect to see, effectively, no material stretching and, hence, $\lambda_\varphi = \lim_{\sigma\to\infty} r_0[s(\sigma)]/r_0(\sigma) \approx r_0(\sigma)/r_0(\sigma) = 1$. It is important to note, however, that the functional relationship (10) is nonlocal since the arclength $s(\sigma)$ is determined by integration of the metric along the curve up to the given point σ.

However, this self-similar ansatz maybe explored analytically in a quite straightforward way by simply expanding all the dependent variables in Taylor series of the form

$$r = \sum_{i=2}^{\infty} r_i \sigma^i, \quad \theta = \sum_{i=1}^{\infty} \theta_i \sigma^i, \quad s = \sum_{i=1}^{\infty} s_i \sigma^i, \quad r_0 = \sum_{i=2}^{\infty} \rho_i \sigma^i. \tag{11}$$

Substitution of these expansions into the system (7) and (8) together with the constraint (10) yields a closed set of algebraic relationships for the expansion coefficients. Here, for computational simplicity, we use a simpler renormalized pressure field and choose a limiting form of (9), namely, $p = p_{\max}$, $0 \leq \sigma \leq \sigma_1$; $p = 0$, $\sigma > \sigma_1$, thereby making the membrane completely rigid outside the apical expansion zone $0 \leq \sigma \leq \sigma_1$. The outer profile is then a cylinder of radius $r(\sigma_1)$ and we can solve for the inner solution. The equations for the coefficients of the Taylor series are closed by requiring that the inner and outer solutions match, that is, $\theta(\sigma_1) = \pi/2$. A typical computation of a self-similar solution is shown in Fig. 6. The closeness of the self-similar solution to the growing solution is striking. The analysis of the self-similar profile for various values of the physical parameters (size of

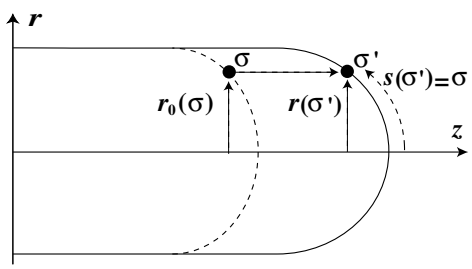

FIG. 5. Self-similar growth ansatz.

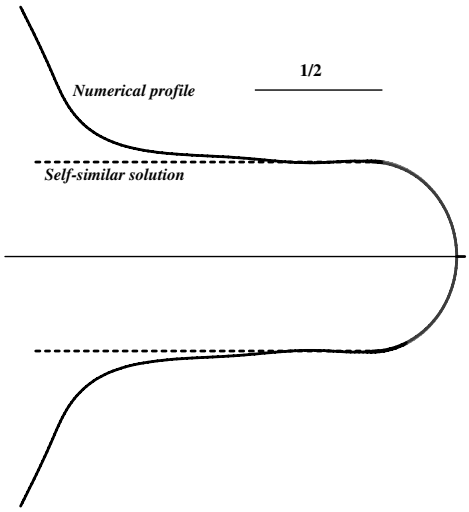

FIG. 6. Comparison of growing membrane profile with self-similar solution. The outermost profile is obtained numerically (in similar fashion as the profiles obtained in Fig. 4 but for $\mu = 1/2$, $\sigma_1 = \pi/6$, $P = A = 1$, $\alpha = 1/64$, $\beta = 10^{-2}$). The inner profile (dashed line) corresponds to the self-similar solution with the same parameter values.

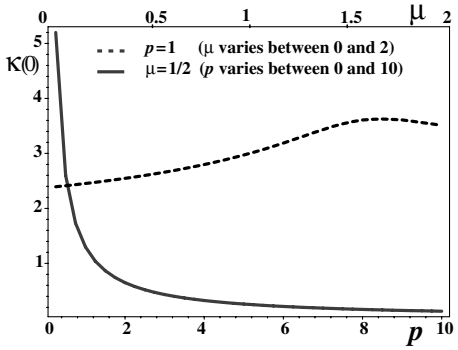

FIG. 7. Curvature at the tip for the self-similar solution ($\sigma_1 = \pi/6$) as a function of the ratio of elastic moduli μ with $p = 1$ constant (dashed line) and as a function of the turgor pressure p at constant μ.

extension zone σ_1, ratio of elastic moduli μ, and effective pressure p) reveal that there is no universal tip shape that can be fitted to all growing fingers. For instance, the curvature at the tip (given by θ_1/ρ_1) varies with all parameters but especially with pressure and elastic moduli (see Fig. 7). Other computations (not shown here) with variants of the effective pressure field all show the same phenomenon of self-similar behavior. The analytical solutions determined by the use of the expansions (11) in the governing Eqs. (7) and (8) are self-similar by imposition of the constraint (10). That the numerical solutions (shown in Fig. 4) generated by the original system (7) and (8) plus growth, but without imposition of (10), exhibit self-similar tip propagation is a reflection of the form of the effective pressure profile (9). If this form is modified to allow for a very "soft" tip, apical swelling is observed. This effect is, in fact, consistent with the observed phenomenon of lysis which occurs when certain enzymes strip the cell wall structure. (A further discussion of lysis within the framework of our model is given in [12]).

The modeling of vegetative actinomycete growth described here indicates that the use of large-deformation theory for elastic membranes (which has been used successfully for studying red blood cell deformation [13]) can provide a satisfactory biomechanical description of pressure driven apical growth. The use of geometry dependent moduli appears capable of providing a biophysically plausible representation of the long-held observation that the "softest" portion of the organism—and, hence, the most susceptible to expansion—is at the tip. This, coupled with a simple mathematical representation of growth through surface reparametrization, enables a simulation of continuous, self-similar, tip expansion that is a realistic depiction of the experimental observations.

We thank N. Mendelson for providing technical advice and laboratory facilities, Dave Bentley for invaluable help with microscopy, and Liz Wellington for providing the bacterial sample. A. G. is supported by the Sloan foundation and a Faculty Small Grant from the University of Arizona. This work is supported by the NSF Grant No. DMS-9972063 (A. G.).

*Electronic address: goriely@math.arizona.edu
URL: http://www.math.arizona.edu/~goriely
†Electronic address: tabor@math.arizona.edu

[1] *Perspective in Physics: Dynamics of curved fronts*, edited by P. Pelcé (Academic Press, San Diego, 1988).
[2] J. I. Prosser and A. J. Tough, Crit. Rev. Biotechnol. **10**, 253 (1991).
[3] N. P. Money, Fungal Genet. Biol. **21**, 173 (1997).
[4] A. P. J. Trinci and P. T. Saunders, J. Gen. Microbiol. **103**, 243 (1977).
[5] S. Bartnicki-Garcia, F. Hergert, and G. Gierz, Protoplasma **153**, 46 (1989).
[6] A. L. Koch, in *Bacterial Growth and Form*, edited by A. L. Koch (Chapman and Hall, New York, 1995), pp. 137–150.
[7] A. E. Green and J. E. Adkins, *Large Elastic Deformations* (Clarendon, Oxford, 1970).
[8] A. Goriely, G. Karolyi, and M. Tabor, "Growth Induced Contour Dynamics," 2002 (to be published).
[9] E. E. Evans and R. Skalak, *Mechanics and Thermodynamics of Biomembranes* (CRC Press Inc., Boca Raton, Florida, 1980).
[10] R. Skalak, A. Tozeren, R. P. Zarda, and S. Chien, Biophys. J. **13**, 245 (1973).
[11] D. I. Gray, G. W. Gooday, and J. I. Prosser, J. Gen. Microbiol. **136**, 1077 (1990).
[12] A. Goriely and M. Tabor, J. Theor. Biol. (to be published).
[13] T. W. Secomb and R. Hsu, Trans. ASME **118**, 536 (1996).